

Electronic and Superconducting Properties of Some FeSe-based Single Crystals and Films Grown Hydrothermally

Xiaoli Dong^{1,2,3*}, Fang Zhou^{1,2,3}, and Zhongxian Zhao^{1,2,3}

¹ Beijing National Laboratory for Condensed Matter Physics and Institute of Physics, Chinese Academy of Sciences, Beijing 100190, China

² University of Chinese Academy of Sciences, Beijing 100049, China

³ Songshan Lake Materials Laboratory, Dongguan, Guangdong 523808, China

* Correspondence to: dong@iphy.ac.cn

Keywords: iron selenide superconductors, superconducting and normal-state properties, spin nematicity, electronic phase separation, high critical parameters, and hydrothermal growth.

Abstract

Our recent year's studies of the prototypal FeSe and molecule-intercalated (Li,Fe)OHFeSe superconductor systems are briefly reviewed here, with emphasis on experimental observations of the link between the superconductivity and normal-state electronic property in the single crystals and films. These samples were successfully synthesized by our recently developed soft-chemical hydrothermal methods, which are also briefly described. Particularly in the Mn-doped high- T_c (Li,Fe)OHFeSe film, a strong enhancement of the superconducting critical current density was achieved, which is promising for practical application of the superconductivity.

1. Introduction

Iron-based superconductors [1] have received extensive attention because of their rich physics, including magnetic and nematic instabilities, electronic correlations, and quantum phenomena [2-9]. As the second class of high- T_c materials after the discovery of cuprate superconductors, the iron-based superconductors are also promising for practical application owing to their large critical current density, high upper critical field, and small anisotropy [10-17]. The recent observation of Majorana zero modes in iron-based superconductors implies a potentiality for future application in topological quantum calculating [18-21]. Unlike an electronic configuration of Cu-3d⁹ in the cuprates, the iron-based compounds have an electronic configuration of Fe-3d⁶ and a small crystal-field splitting [2,7,22-24]. An immediate consequence of this is that all the five Fe-3d orbitals could be involved in the low-energy interactions [25], giving rise to the multiband nature of the iron-based superconductivity, and the complexity and multiplicity of the normal-state properties. The iron-based family has two major subclasses, the iron chalcogenide and pnictide superconductors. Among them, the iron selenide superconductors have been shown to display a highly tunable superconducting critical T_c and unique electronic properties in the normal state, thus providing a superior platform to investigate the underlying physics for iron-based superconductivity.

Superconductivity of FeSe-based compounds emerges from the layered blocks formed by edge-sharing FeSe-tetrahedra, each containing one iron-plane sandwiched between two selenium-planes. An important feature is that the superconducting T_c can be tuned in a wide range. The simplest binary FeSe shows bulk superconductivity at a lower $T_c \sim 9$ K under ambient pressure [26]. It is notable that T_c can be boosted to tens of kelvin (30 K – 50K), by the applications of high pressure [27-33], charge-carrier injection[34], electrochemical etching [35], and chemical intercalation. The weak van der Waals bonding between the neighboring FeSe-blocks allows a variety of FeSe-based intercalates to be obtained, such as the atom-intercalated $A_y\text{Fe}_{2-x}\text{Se}_2$ (A =alkali metal) [36-40], molecule-intercalated $(\text{Li}_{0.8}\text{Fe}_{0.2})\text{OHFeSe}$ [41], and atom/molecule-co-intercalated $\text{Li}_x(\text{C}_5\text{H}_5\text{N})_y\text{Fe}_{2-z}\text{Se}_2$ [42], $\text{A}_x(\text{NH}_2)_y(\text{NH}_3)_{1-y}\text{Fe}_2\text{Se}_2$ [43,44], $\text{A}_x(\text{NH}_3)_y\text{Fe}_2\text{Se}_2$ [45-47] and $\text{A}_x(\text{C}_2\text{H}_8\text{N}_2)_y\text{Fe}_2\text{Se}_2$ [48]. Moreover, the highest superconducting gap opening temperature (~ 65 K) among all the iron-based superconductors has been observed in a monolayer FeSe grown on a SrTiO_3 substrate [49,50]. On the other hand, distinct from most iron-based superconductor systems, FeSe does not order magnetically at ambient pressure. However, a unique electronic nematic order has been observed to develop in FeSe, which is associated with a rotational-symmetry-breaking transition from a tetragonal to an orthorhombic phase at $T_s \sim 90$ K [51,52]. The electronic nematicity is directly related to a degeneracy lifting of the bands with Fe 3d_{xz} and 3d_{yz} orbital characters [53-55]. Compared to the Fermi-surface topology of the prototypal FeSe, in the molecule-intercalated $(\text{Li,Fe})\text{OHFeSe}$ single crystals, only the electron pockets near the Brillouin zone corners are observed, in absence of the hole pocket near the zone center [56,57]. This raises question about a proposed pairing scenario of the electronic scatterings between the hole-like and electron-like pockets. Study of the FeSe-based superconductors is essential for a better understanding of the unconventional superconductivity.

To investigate the link between the unconventional superconductivity and unusual normal-state electronic properties, and the potential for the superconductivity application, high-quality single crystal and film samples are highly demanded. Recent years, we have been exploring soft-chemical methods suitable for synthesizing the FeSe-based superconductor single crystals and single-crystalline films hard to obtain by conventional high-temperature growth. By developing hydrothermal ion-exchange [58-60] and ion-deintercalation [61,62] approaches, we have succeeded in synthesizing series of high-quality sizable single crystals of the intercalated $(\text{Li,Fe})\text{OHFeSe}$ and

binary FeSe systems, respectively. Our further study [9] has shown a strong electronic two-dimensionality and a nearly linear extracted magnetic susceptibility in the hydrothermal high- T_c (42 K) (Li,Fe)OHFeSe single crystal, suggesting the presence of two-dimensional magnetic fluctuations in the normal state. In a series of the (Li, Fe)OHFeSe single crystals, a coexistence of antiferromagnetism with superconductivity has been detected [60]. We explain such coexistence by electronic phase separation, similar to the previously observed in high- T_c cuprates and iron arsenides. An electronic phase diagram is further established for (Li, Fe)OHFeSe system [60,63]. In hydrothermal binary Fe_{1-x}Se single crystals, we have observed a field-induced two-fold rotational symmetry emerging below T_{sn} in angular-dependent magnetoresistance measurements, and a linear relationship between T_c and T_{sn} [61,64]. Importantly, we find in our recent study [9] that the superconductivity of FeSe system emerges from the strongly correlated, hole-dominated Fe_{1-x}Se as the non-stoichiometry is reduced to $x \sim 5.3\%$. Interestingly, such an x threshold for superconductivity of the prototypal FeSe is similar to that ($x \sim 5\%$ [65]) for high- T_c superconductivity of the intercalated (Li, Fe)OHFeSe sharing the common superconducting FeSe-blocks.

We have also succeeded in synthesizing a series of high-quality single-crystalline films of (Li, Fe)OHFeSe system, by inventing a hydrothermal epitaxial film technique [16,17,66]. We find that doping Mn into high- T_c (Li, Fe)OHFeSe films can raise the superconducting critical current density J_c by one order of magnitude to 0.32 MA/cm^2 at a high field of 33 T [17]. Such a high J_c value is the record so far among the iron-based superconductors, and is thus promising for high-field application of the superconductivity. Besides, our breakthrough in the crystal growth has greatly promoted other related studies and progresses have been made [57,59,60,67-71], including the ARPES study of Fermi-surface topology [57] and the observation of pressure-induced second high- T_c ($> 50 \text{ K}$) phase [70] in the (Li,Fe)OHFeSe system. Our developed growth method has also been adopted in the studies of other research groups [56,72-83].

2. Soft-chemical hydrothermal growth methods developed for FeSe-based single crystals and films

The discovery of $\text{Li}_{0.8}\text{Fe}_{0.2}\text{OHFeSe}$ (FeSe-11111) superconductor [41] brings new opportunity for the study of iron-based superconductivity. (Li, Fe)OHFeSe is free from the complications of the structural transition, associated with the electronic nematicity, and the chemical phase separation, related to the inter-grown insulating $\text{K}_{0.8}\text{Fe}_{1.6}\text{Se}_2$ (KFS-245 phase) [63], as compared to the prototypal FeSe-11 and $\text{K}_{1-y}\text{Fe}_{2-x}\text{Se}_{2-122}$ superconductors, respectively. Moreover, it shows an ambient-pressure high $T_c = 42 \text{ K}$ and a pressure-induced higher $T_c > 50 \text{ K}$ under 12.5 GPa [70]. Having a Fermi-surface topology [56,57] similar to the high- T_c ($> 65 \text{ K}$) FeSe monolayer, (Li, Fe)OHFeSe system turns out to be an ideal platform for studying the superconducting and normal-state properties of high- T_c iron-based superconductors. Initially, only the powder samples of (Li, Fe)OHFeSe can be prepared hydrothermally [41,63,65,84,85]. For in-depth investigations on the intrinsic and anisotropic physical properties, the high-quality single crystal and film samples are indispensable.

The crystal structure of (Li, Fe)OHFeSe consists of a stacking of one superconducting (SC) FeSe-block alternating with one insulating (Li, Fe)OH-block along the c -axis. The (Li, Fe)OHFeSe compound suffers an easy decomposition because of the inherent weak hydrogen bonding. Therefore, none of the conventional high-temperature methods is applicable to grow the single crystals. To overcome this problem, we have developed a soft-chemical hydrothermal ion-exchange method capable of producing high-quality sizable single crystals of (Li, Fe)OHFeSe [58]. For the

hydrothermal ion-exchange reaction, large and high-quality $\text{K}_{0.8}\text{Fe}_{1.6}\text{Se}_2$ crystal is used as a kind of matrix. The structure of $\text{K}_{0.8}\text{Fe}_{1.6}\text{Se}_2$ is formed by alternatively stacked K-layer and FeSe-tetrahedron-block similar to the target compound. The K ions in $\text{K}_{0.8}\text{Fe}_{1.6}\text{Se}_2$ are completely de-intercalated during the hydrothermal process. Simultaneously, the (Li, Fe)OH-blocks constructed by ions from the hydrothermal solution are intercalated into the matrix, and the ordered vacant Fe-sites (20% in amount) originally in the matrix $\text{Fe}_{0.8}\text{Se}$ -blocks are almost occupied. A series of large and high-quality (Li, Fe)OHFeSe single crystals [60] are thus derived. Fig. 1 schematically illustrates the hydrothermal ion-exchange process. The derived (Li, Fe)OHFeSe single crystal almost inherits the original shape of the matrix (insets of Fig. 1b, c). Inspired by the successful hydrothermal ion-exchange method for the single crystals, we have further invented a hydrothermal epitaxial film technique to fabricate a series of high-quality single-crystalline films of un-doped [66] and Mn-doped [17] (Li, Fe)OHFeSe showing an optimal zero-resistivity $T_c = 42.4$ K. This series of high-quality (Li, Fe)OHFeSe films has enabled a systematic study of the superconducting and normal-state properties [66].

By modifying the hydrothermal reaction conditions, we have also developed a hydrothermal ion-deintercalation (HID) method, as illustrated in Fig. 2. The atomic ratio of the FeSe-blocks can be continuously tuned by the HID process, yielding a series of non-stoichiometric Fe_{1-x}Se single crystals at various charge-doping levels [9,61,62]. FeSe crystals used to be grown by chemical-vapor-transport [86,87], flux-free floating-zone [88], and flux solution methods. These methods are usually hard to tune the chemical stoichiometry.

3. Electronic and superconducting properties studied in the hydrothermal single crystals and films

Now we briefly review our recent year's studies of the series of FeSe-based single crystals and films grown by the hydrothermal methods.

3.1 Strong electronic two-dimensionality in high- T_c (Li,Fe)OHFeSe single crystal

Fig.3a shows the temperature dependence of the in-plane resistivity, ρ_{ab} , for the high- T_c (42 K) $(\text{Li}_{0.84}\text{Fe}_{0.16})\text{OHFe}_{0.98}\text{Se}$ single crystal [58], which displays a metallic behavior over the whole measuring temperature range in the normal state. As a measure of the charge transport anisotropy, the ratio of the out-of-plane to in-plane resistivity, ρ_c/ρ_{ab} , was found to increase with lowering temperature and reach a high value of 2500 at 50 K. It is obvious that the normal-state electronic property turns out to be highly two dimensional just above T_c . Shown in Fig. 3b is the temperature dependence of static magnetic susceptibility, which is slightly dependent on the magnitude of the applied field. In the higher temperature range, all the data can be fitted to a modified Curie-Weiss law $\chi_m = \chi_0 + \chi_{\text{CW}}$ (the solid lines), where χ_0 is the Pauli paramagnetic contribution from itinerant charge carriers. A deviation from the Curie-Weiss law is clearly visible below a characteristic T^* (~ 120 K) of a Hall-coefficient dip feature, coinciding with the upturn in Hall coefficient and change in the resistivity behavior. From the Hall-dip T^* down to the superconducting T_c , both the extracted iron-plane magnetic susceptibility (with the Curie-Weiss term subtracted; inset of Fig. 3b) and the in-plane resistivity (inset of Fig. 3a) exhibit a linear temperature dependence, suggesting the presence of two-dimensional antiferromagnetic spin fluctuations in the iron planes.

3.2 Phase diagram and electronic phase separation of (Li,Fe)OHFeSe system

The first phase diagram of (Li, Fe)OHFeSe system [63] was based on the powder samples. In a subsequent work [60], we established a more complete phase diagram for the system (Fig. 4), based

on a series of the hydrothermal single crystals in the superconducting (SC) and non-superconducting regimes. In some of the SC samples ($T_c < \sim 38$ K, cell parameter $c < \sim 9.27$ Å), we observed a strong drop in the magnetization at an almost constant temperature scale $T_{\text{afm}} \sim 125$ K (Fig. 5a, b), indicating the occurrence of antiferromagnetism well above T_c . Our analysis of electron energy-loss spectroscopy combined with selected-area electron diffraction confirmed the absence of magnetic impurity phases such as Fe_3O_4 . Therefore, the antiferromagnetic signal is intrinsic to (Li, Fe)OHFeSe system. Moreover, a positive correlation between the sizes of the antiferromagnetic signal and the Meissner signal was observed (Fig. 5c and d). These experimental results demonstrate the coexistence of an antiferromagnetic state with the superconducting state in (Li, Fe)OHFeSe at $T_c < \sim 38$ K and $c < \sim 9.27$ Å. Such coexistence can be explained by electronic phase separation [60], similar to the cases of high- T_c cuprates and iron arsenides. Therefore the electronic phase diagram shown in Fig. 4 provides more information about the electronic states in (Li, Fe)OHFeSe system.

3.3 The link between the superconducting and normal-state properties in Fe_{1-x}Se single crystals

The in-plane angular-dependent magnetoresistance (AMR) in the normal state was measured for the hydrothermal Fe_{1-x}Se single crystals [64]. Fig. 6 shows the AMR at a 9 Tesla field for a representative sample with $T_c = 7.6$ K. The AMR displays a two-fold rotational symmetry emerging below a characteristic temperature $T_{\text{sn}} \sim 55$ K. This anisotropy in AMR is enhanced with decreasing temperature (left panel of Fig. 6). Such an enhancement in charge scatterings was also observed in the temperature-dependent magnetoresistance by an earlier study [89]. Moreover, a downward curvature below $T_{\text{sn}} \sim 55$ K was observed in our sample in the static magnetization under an in-plane magnetic field of 0.1 T (Fig. 7a) [61]. Such a feature is strongly dependent on the magnitude and direction of the applied field (Fig. 7a vs. b). This suggests that the strong quantum spin frustrations predominate in the iron planes. Although the orbital-nematic order associated with the structural transition at $T_s \sim 90$ K is also of a two-fold rotational symmetry, the obvious downward feature of in-plane static magnetization below $T_{\text{sn}} \sim 55$ K, which is far below T_s , suggests that the fourfold-rotational-symmetry breaking identified by our AMR measurements is closely related to the frustrated spins with anisotropic magnetic fluctuations. Therefore, a field-induced nematic state of a spin origin emerges below T_{sn} .

By summarizing all the data of our samples, we found a remarkable linear relationship between T_c and T_{sn} , as shown in Fig. 8. Moreover, the related data of T_c vs. T_{sn} available from literature [89-91] also well satisfy this linear relationship. Namely, the linear relationship between superconducting T_c and characteristic T_{sn} of the field-induced spin-nematic state was observed to cover a wide range from far below to beyond T_s . This further suggests that the superconductivity is more likely related to the anisotropic magnetic fluctuations. These results of prototypal FeSe system are consistent with those of intercalated high- T_c (Li,Fe)OHFeSe presented above. It needs to be emphasized that, for nearly stoichiometric FeSe samples with a constant $T_c \sim 9.5$ K, both the spin-nematic ordering and orbital-nematic ordering (associated with the structural transition) happen to coincide with each other at ~ 90 K, as shown in Fig. 8. So it is difficult to distinguish these different ordering states in such samples. Our samples with different T_c 's enable the disentanglement of the different states.

Most recently, we have studied the doping dependences of electronic correlation effect [9] and upper critical field behavior [62] in a series of hydrothermal Fe_{1-x}Se single crystals. Particularly in these binary Fe_{1-x}Se samples, the charge-doping level can be tuned simply by the non-stoichiometric x of Fe, from a strong electron dominance at $x \sim 0$ to a strong hole dominance at higher x values. Importantly, we find that superconductivity of FeSe system emerges from the strongly correlated, hole-dominated Fe_{1-x}Se as the non-stoichiometry is reduced to $x \sim 5.3$ % [9]. Interestingly, such an x

threshold for superconductivity of the prototypal FeSe is similar to that ($x \sim 5\%$ [65]) for high- T_c superconductivity of the intercalated (Li, Fe)OHFeSe sharing the common superconducting FeSe-blocks.

3.4 High superconducting critical parameters of un-doped and Mn-doped (Li,Fe)OHFeSe crystals and films

Fig. 9 shows the x-ray diffraction characterization of a representative (Li,Fe)OHFeSe film sample hydrothermally grown on LaAlO_3 substrate [16]. The observation of only (00 l) reflections indicates a single preferred (001) orientation (Fig. 9a). Shown in Fig. 9b is the double-crystal x-ray rocking curve for the (006) Bragg reflection, with a small FWHM = 0.22° . To our knowledge, this is the best FWHM value observed so far among various iron-based superconductor crystals and films, indicating a high sample quality. The ϕ -scan of (101) plane shown in Fig. 9c exhibits four successive peaks with an equal interval of 90° , consistent with the C_4 symmetry of the (Li,Fe)OHFeSe film. These results clearly demonstrate an excellent in-plane orientation and epitaxial growth.

High-quality superconducting films can play an important role in the application. Besides the high sample quality, the (Li,Fe)OHFeSe films also display excellent superconducting properties. The temperature dependence of in-plane resistivity is shown in Fig. 10a, with a superconducting zero-resistivity temperature up to 42.4 K. Fig. 10b is the temperature dependences of upper critical field H_{c2} derived from systematic measurements of the in-plane and out-of-plane magnetoresistance. Based on WHH (Werthamer-Helfand-Hohenberg) model, the values of $H_{c2}(0)$ are estimated as 79.5 T and 443 T at magnetic fields perpendicular and parallel to the ab plane, respectively. Moreover, a large critical current density $J_c > 0.5 \text{ MA/cm}^2$ was achieved at ~ 20 K, as shown in Fig. 10c. The high superconducting critical parameters are important for practical application. Additionally, as seen from Fig. 11, the critical temperature T_c of $(\text{Li}_{0.84}\text{Fe}_{0.16})\text{OHFe}_{0.98}\text{Se}$ single crystal can be further raised up to a value > 50 K under a pressure of 12.5 GPa, in the superconducting phase II (SC-II) region. The SC-II phase develops with pressure at a critical $P_c = 5$ GPa as the superconducting phase I (SC-I) is gradually suppressed.

Very recently, we have successfully doped Mn into (Li,Fe)OHFeSe films [17]. As seen from Fig. 12a, the J_c value of high- T_c (Li,Fe)OHFeSe film is strongly enhanced by one order of magnitude, from the undoped 0.03 to Mn-doped 0.32 MA/cm^2 under 33 T at 5 K. The vortex pinning force density F_p monotonically increases with field up to 106 GN/m^3 , shown in Fig. 12b. To the best of our knowledge, these values are the records so far among all the iron-based superconductors. Such a superconducting (Li,Fe)OHFeSe film is not only important for the fundamental research, but also promising for high-field application.

4. Conclusion

High-quality single crystals and single-crystalline films of iron-based superconductors play an important role in both the basic research and potential application. However, for the FeSe-based superconductor systems reviewed here, by the conventional high-temperature growth it is either hard to obtain the single crystals and films, or not easy to tune the electronic properties. These problems can be overcome by our recently developed soft-chemical hydrothermal growth methods, which are capable of producing the single crystals and films, and tuning the chemical stoichiometry thus the electronic properties. In addition, these methods may be applicable in other layered materials, providing a new route for the exploration of functional materials.

The successful crystal and film growth has enabled systematic studies of the FeSe-based superconductor systems. We have observed a strong electronic two-dimensionality towards T_c , and a nearly linear extracted magnetic susceptibility as well as a linear in-plane resistivity, both emerging from a characteristic T^* (~ 120 K) of a Hall-coefficient dip feature down to T_c , in high- T_c intercalated (Li,Fe)OHFeSe system. We have also observed a linear relationship between T_c and a characteristic T_{sn} of a field-induced spin nematicity in prototypal FeSe system. These results suggest the presence of magnetic fluctuations in the iron planes and their relevance to superconductivity. Importantly, we have found that superconductivity of the prototypal FeSe emerges from the strongly correlated, hole-dominated Fe_{1-x}Se at a non-stoichiometric x similar to that for the high- T_c superconductivity of the FeSe-intercalate (Li, Fe)OHFeSe. An electronic phase diagram has been established for (Li, Fe)OHFeSe system, with the coexistence of antiferromagnetism and superconductivity explained by electronic phase separation. On the other hand, the high superconducting critical current density achieved in Mn-doped high- T_c (Li,Fe)OHFeSe film is promising for high-field application. These FeSe-based superconductor systems deserve further experimental and theoretical studies, in both aspects of the underlying physics and potential application.

Conflict of Interest

The authors declare that the research was conducted in the absence of any commercial or financial relationships that could be construed as a potential conflict of interest.

Author contributions

All authors contribute to the writing of the manuscript.

Funding

This work was supported by National Natural Science Foundation of China (Nos. 11834016 and 11888101), the National Key Research and Development Program of China (Grant Nos. 2017YFA0303003, 2016YFA0300300), and the Strategic Priority Research Program and Key Research Program of Frontier Sciences of the Chinese Academy of Sciences (Grant Nos. XDB25000000, QYZDY-SSW-SLH001)

ACKNOWLEDGMENTS

We are very thankful to all our collaborators for their valuable scientific contributions in the past six years, especially Huaxue Zhou, Dongna Yuan, Yulong Huang, Yiyuan Mao, Shunli Ni, Jinpeng Tian, Dong Li, and Peipei Shen for sample preparation and characterization. We are also very grateful to Kui Jin, Jie Yuan, Wei Hu, and Zhongpei Feng for electrical transport measurements and insightful discussions; Jinguang Cheng and Jianping Sun for high-pressure research; Zian Li, Huaixin Yang, and Jianqi Li for TEM & EELS studies; Guangming Zhang and Zhenyu Zhang for theoretical support; Xingjiang Zhou and Lin Zhao for ARPES studies; Donglai Feng and Tong Zhang for STM studies; Li Pi, Chuanying Xi, Zhaosheng Wang, and J. Wosnitza for high-field studies; Rustem Khasanov, Zurab Guguchia, and Alex Amato for μ SR studies. We also thank Ping Zheng, Shaokui Su, and Lihong Yang for technical supports.

Reference

- 1 Y. Kamihara, T. Watanabe, M. Hirano, and H. Hosono, "Iron-based layered superconductor LaO_{1-x}F_xFeAs ($x=0.05-0.12$) with $T_c=26$ K," J. Am. Chem. Soc. **130**, 3296 (2008).
- 2 D. C. Johnston, "The puzzle of high temperature superconductivity in layered iron pnictides and chalcogenides," Adv. Phys. **59**, 803 (2010).
- 3 Igor I. Mazin, "Superconductivity gets an iron boost," Nature **464**, 183 (2010).
- 4 J. Paglione and R. L. Greene, "High-temperature superconductivity in iron-based materials," Nat. Phys. **6**, 645 (2010).
- 5 G. R. Stewart, "Superconductivity in iron compounds," Rev. Mod. Phys. **83**, 1589 (2011).
- 6 E. Dagotto, "Colloquium: the unexpected properties of alkali metal iron selenide superconductors," Rev. Mod. Phys. **85**, 849 (2013).
- 7 Xianhui Chen, Pengcheng Dai, Donglai Feng, Tao Xiang, and Fu-Chun Zhang, "Iron-based high transition temperature superconductors," National Science Review **1**, 371 (2014).
- 8 Takasada Shibauchi, Tetsuo Hanaguri, and Yuji Matsuda, "Exotic Superconducting States in FeSe-based Materials," arXiv2005.07315 (2020).

- 9 S. L. Ni, J. P. Sun, S. B. Liu, J. Yuan, Li Yu, M. W. Ma, L. Zhang, L. Pi, P. Zheng, P. P. Shen, D. Li, D. E. Shi, G. B. Li, J. L. Sun, G. M. Zhang, K. Jin, J. -G. Cheng, F. Zhou, X. L. Dong, and Z. X. Zhao, "Emergence of superconductivity in strongly correlated hole-dominated Fe_{1-x}Se," arxiv1912.12614 (2019).
- 10 M. Putti, I. Pallecchi, E. Bellingeri, M. R. Cimberle, M. Tropeano, C. Ferdeghini, A. Palenzona, C. Tarantini, A. Yamamoto, J. Jiang, J. Jaroszynski, F. Kametani, D. Abraimov, A. Polyanskii, J. D. Weiss, E. E. Hellstrom, A. Gurevich, D. C. Larbalestier, R. Jin, B. C. Sales, A. S. Sefat, M. A. McGuire, D. Mandrus, P. Cheng, Y. Jia, H. H. Wen, S. Lee, and C. B. Eom, "New Fe-based superconductors: properties relevant for applications," *Supercond. Sci. Tech.* **23**, 034003 (2010).
- 11 Q. Li, W. D. Si, and I. K. Dimitrov, "Films of iron chalcogenide superconductors," *Rep. Prog. Phys.* **74**, 124510 (2011).
- 12 Yanwei Ma, "Progress in wire fabrication of iron-based superconductors," *Supercond. Sci. Tech.* **25**, 113001 (2012).
- 13 S. Haindl, M. Kidszun, S. Oswald, C. Hess, B. Büchner, S. Köling, L. Wilde, T. Thersleff, V. V. Yurchenko, M. Jourdan, H. Hiramatsu, and H. Hosono, "Thin film growth of Fe-based superconductors: from fundamental properties to functional devices. A comparative review," *Rep. Prog. Phys.* **77**, 046502 (2014).
- 14 H. Hosono, K. Tanabe, E. Takayama-Muromachi, H. Kageyama, S. Yamanaka, H. Kumakura, M. Nohara, H. Hiramatsu, and S. Fujitsu, "Exploration of new superconductors and functional materials, and fabrication of superconducting tapes and wires of iron pnictides," *Sci. Technol. Adv. Mater.* **16**, 033503 (2015).
- 15 J. Hänisch, K. Iida, R. Huehne, and C. Tarantini, "Fe-based superconducting thin films-preparation and tuning of superconducting properties," *Supercond. Sci. Tech.* **32**, 093001 (2019).
- 16 Yulong Huang, Zhongpei Feng, Shunli Ni, Jun Li, Wei Hu, Shaobo Liu, Yiyuan Mao, Huaxue Zhou, Fang Zhou, Kui Jin, Huabing Wang, Jie Yuan, Xiaoli Dong, and Zhongxian Zhao, "Superconducting (Li,Fe)OHFeSe Film of High Quality and High Critical Parameters," *Chin. Phys. Lett.* **34**, 077404 (2017).
- 17 Dong Li, Jie Yuan, Peipei Shen, Chuanying Xi, Jinpeng Tian, Shunli Ni, Jingsong Zhang, Zhongxu Wei, Wei Hu, Zian Li, Li Yu, Jun Miao, Fang Zhou, Li Pi, Kui Jin, Xiaoli Dong, and Zhongxian Zhao, "Giant enhancement of critical current density at high field in superconducting (Li,Fe)OHFeSe films by Mn doping," *Supercond. Sci. Tech.* **32**, 12LT01 (2019).
- 18 Dongfei Wang, Lingyuan Kong, Peng Fan, Hui Chen, Shiyu Zhu, Wen Yao Liu, Lu Cao, Yujie Sun, Shixuan Du, John Schneeloch, Ruidan Zhong, Genda Gu, Liang Fu, Hong Ding, and Hong-Jun Gao, "Evidence for Majorana bound states in an iron-based superconductor," *Science* **362**, 333 (2018).
- 19 Peng Zhang, Koichiro Yaji, Takahiro Hashimoto, Yuichi Ota, Takeshi Kondo, Kozo Okazaki, Zhijun Wang, Jinsheng Wen, G. D. Gu, Hong Ding, and Shik Shin, "Observation of topological superconductivity on the surface of an iron-based superconductor," *Science* **360**, 182 (2018).
- 20 Qin Liu, Chen Chen, Tong Zhang, Rui Peng, Ya-Jun Yan, Chen-Hao-Ping Wen, Xia Lou, Yu-Long Huang, Jin-Peng Tian, Xiao-Li Dong, Guang-Wei Wang, Wei-Cheng Bao, Qiang-

- Hua Wang, Zhi-Ping Yin, Zhong-Xian Zhao, and Dong-Lai Feng, "Robust and Clean Majorana Zero Mode in the Vortex Core of High-Temperature Superconductor (Li_{0.84}Fe_{0.16})OHFeSe," *Phys. Rev. X* **8**, 041056 (2018).
- 21 C. Chen, Q. Liu, T. Z. Zhang, D. Li, P. P. Shen, X. L. Dong, Z. X. Zhao, T. Zhang, and D. L. Feng, "Quantized Conductance of Majorana Zero Mode in the Vortex of the Topological Superconductor (Li_{0.84}Fe_{0.16})OHFeSe," *Chin. Phys. Lett.* **36**, 057403 (2019).
 - 22 Chao Cao, P. J. Hirschfeld, and Hai-Ping Cheng, "Proximity of antiferromagnetism and superconductivity in LaFeAsO_{1-x}F_x: Effective Hamiltonian from ab initio studies," *Phys. Rev. B* **77**, 220506R (2008).
 - 23 Qimiao Si and Elihu Abrahams, "Strong Correlations and Magnetic Frustration in the High T_c Iron Pnictides," *Phys. Rev. Lett.* **101**, 076401 (2008).
 - 24 Zhong-Yi Lu, Fengjie Ma, and Tao Xiang, "Pnictogen-bridged antiferromagnetic superexchange interactions in iron pnictides," *J. Phys. Chem. Solids* **72**, 319 (2011).
 - 25 R. M. Fernandes, A. V. Chubukov, and J. Schmalian, "What drives nematic order in iron-based superconductors?," *Nat. Phys.* **10**, 97 (2014).
 - 26 F. C. Hsu, J. Y. Luo, K. W. Yeh, T. K. Chen, T. W. Huang, P. M. Wu, Y. C. Lee, Y. L. Huang, Y. Y. Chu, D. C. Yan, and M. K. Wu, "Superconductivity in the PbO-type structure α -FeSe," *Proc. Natl. Acad. Sci.* **105**, 14262 (2008).
 - 27 Yoshikazu Mizuguchi, Fumiaki Tomioka, Shunsuke Tsuda, Takahide Yamaguchi, and Yoshihiko Takano, "Superconductivity at 27K in tetragonal FeSe under high pressure," *Appl. Phys. Lett.* **93**, 152505 (2008).
 - 28 S. Margadonna, Y. Takabayashi, Y. Ohishi, Y. Mizuguchi, Y. Takano, T. Kagayama, T. Nakagawa, M. Takata, and K. Prassides, "Pressure evolution of the low-temperature crystal structure and bonding of the superconductor FeSe (T_c=37K)," *Phys. Rev. B* **80**, 064506 (2009).
 - 29 S. Medvedev, T. M. McQueen, I. A. Troyan, T. Palasyuk, M. I. Erements, R. J. Cava, S. Naghavi, F. Casper, V. Ksenofontov, G. Wortmann, and C. Felser, "Electronic and magnetic phase diagram of beta-Fe_{1.01}Se with superconductivity at 36.7 K under pressure," *Nat. Mater.* **8**, 630 (2009).
 - 30 K. Kothapalli, A. E. Bohmer, W. T. Jayasekara, B. G. Ueland, P. Das, A. Sapkota, V. Taufour, Y. Xiao, E. Alp, S. L. Bud'ko, P. C. Canfield, A. Kreyssig, and A. I. Goldman, "Strong cooperative coupling of pressure-induced magnetic order and nematicity in FeSe," *Nat. Commun.* **7**, 12728 (2016).
 - 31 J. P. Sun, K. Matsuura, G. Z. Ye, Y. Mizukami, M. Shimozawa, K. Matsubayashi, M. Yamashita, T. Watashige, S. Kasahara, Y. Matsuda, J. Q. Yan, B. C. Sales, Y. Uwatoko, J. G. Cheng, and T. Shibauchi, "Dome-shaped magnetic order competing with high-temperature superconductivity at high pressures in FeSe," *Nat. Commun.* **7**, 12146 (2016).
 - 32 Rustem Khasanov, Zurab Guguchia, Alex Amato, Elvezio Morenzoni, Xiaoli Dong, Fang Zhou, and Zhongxian Zhao, "Pressure-induced magnetic order in FeSe: A muon spin rotation study," *Phys. Rev. B* **95**, 180504R (2017).
 - 33 Rustem Khasanov, Rafael M. Fernandes, Gediminas Simutis, Zurab Guguchia, Alex Amato, Hubertus Luetkens, Elvezio Morenzoni, Xiaoli Dong, Fang Zhou, and Zhongxian Zhao,

- "Magnetic tricritical point and nematicity in FeSe under pressure," *Phys. Rev. B* **97**, 224510 (2018).
- 34 B. Lei, J. H. Cui, Z. J. Xiang, C. Shang, N. Z. Wang, G. J. Ye, X. G. Luo, T. Wu, Z. Sun, and X. H. Chen, "Evolution of High-Temperature Superconductivity from a Low-Tc Phase Tuned by Carrier Concentration in FeSe Thin Flakes," *Phys. Rev. Lett.* **116**, 077002 (2016).
 - 35 Naoki Shikama, Yuki Sakishita, Fuyuki Nabeshima, Yumiko Katayama, Kazunori Ueno, and Atsutaka Maeda, "Enhancement of superconducting transition temperature in electrochemically etched FeSe/LaAlO₃ films," arXiv2005.06982 (2020).
 - 36 Jiangang Guo, Shifeng Jin, Gang Wang, Shunchong Wang, Kaixing Zhu, Tingting Zhou, Meng He, and Xiaolong Chen, "Superconductivity in the iron selenide KxFe₂Se₂ (0 ≤ x ≤ 1.0)," *Phys. Rev. B* **82**, 180520R (2010).
 - 37 M. H. Fang, H. D. Wang, C. H. Dong, Z. J. Li, C. M. Feng, J. Chen, and H. Q. Yuan, "Fe-based superconductivity with T_c=31 K bordering an antiferromagnetic insulator in (Tl,K) FexSe₂," *Epl* **94**, 27009 (2011).
 - 38 A. F. Wang, J. J. Ying, Y. J. Yan, R. H. Liu, X. G. Luo, Z. Y. Li, X. F. Wang, M. Zhang, G. J. Ye, P. Cheng, Z. J. Xiang, and X. H. Chen, "Superconductivity at 32 K in single-crystalline RbxFe₂-ySe₂," *Phys. Rev. B* **83**, 060512R (2011).
 - 39 T. P. Ying, X. L. Chen, G. Wang, S. F. Jin, T. T. Zhou, X. F. Lai, H. Zhang, and W. Y. Wang, "Observation of superconductivity at 30 similar to 46K in AxFe₂Se₂ (A=Li, Na, Ba, Sr, Ca, Yb, and Eu)," *Scientific Reports* **2**, 426 (2012).
 - 40 A. M. Zhang, T. L. Xia, K. Liu, W. Tong, Z. R. Yang, and Q. M. Zhang, "Superconductivity at 44 K in K intercalated FeSe system with excess Fe," *Scientific Reports* **3**, 1216 (2013).
 - 41 X. F. Lu, N. Z. Wang, H. Wu, Y. P. Wu, D. Zhao, X. Z. Zeng, X. G. Luo, T. Wu, W. Bao, G. H. Zhang, F. Q. Huang, Q. Z. Huang, and X. H. Chen, "Coexistence of superconductivity and antiferromagnetism in (Li_{0.8}Fe_{0.2})OHFeSe," *Nat. Mater.* **14**, 325 (2014).
 - 42 A. Krzton-Maziopa, E. V. Pomjakushina, V. Y. Pomjakushin, F. von Rohr, A. Schilling, and K. Conder, "Synthesis of a new alkali metal-organic solvent intercalated iron selenide superconductor with T_c approximate to 45 K," *J. Phys-condens. Mat.* **24**, 382202 (2012).
 - 43 M. Burrard-Lucas, D. G. Free, S. J. Sedlmaier, J. D. Wright, S. J. Cassidy, Y. Hara, A. J. Corkett, T. Lancaster, P. J. Baker, S. J. Blundell, and S. J. Clarke, "Enhancement of the superconducting transition temperature of FeSe by intercalation of a molecular spacer layer," *Nat. Mater.* **12**, 15 (2013).
 - 44 Stefan J. Sedlmaier, Simon J. Cassidy, Richard G. Morris, Michael Drakopoulos, Christina Reinhard, Saul J. Moorhouse, Dermot O'Hare, Pascal Manuel, Dmitry Khalyavin, and Simon J. Clarke, "Ammonia-Rich High-Temperature Superconducting Intercalates of Iron Selenide Revealed through Time-Resolved in Situ X-ray and Neutron Diffraction," *J. Am. Chem. Soc.* **136**, 630 (2014).
 - 45 E. W. Scheidt, V. R. Hathwar, D. Schmitz, A. Dunbar, W. Scherer, F. Mayr, V. Tsurkan, J. Deisenhofer, and A. Loidl, "Superconductivity at T_c=44 K in LixFe₂Se₂(NH₃)_y," *Eur. Phys. J. B* **85**, 279 (2012).
 - 46 T. P. Ying, X. L. Chen, G. Wang, S. F. Jin, X. F. Lai, T. T. Zhou, H. Zhang, S. J. Shen, and W. Y. Wang, "Superconducting Phases in Potassium-Intercalated Iron Selenides," *J. Am. Chem. Soc.* **135**, 2951 (2013).

- 47 Shanshan Sun, Shaohua Wang, Rong Yu, and Hechang Lei, "Extreme anisotropy and anomalous transport properties of heavily electron doped $\text{Li}_x(\text{NH}_3)_y\text{Fe}_2\text{Se}_2$ single crystals," *Phys. Rev. B* **96**, 064512 (2017).
- 48 T. Noji, T. Hatakeda, S. Hosono, T. Kawamata, M. Kato, and Y. Koike, "Synthesis and post-annealing effects of alkaline-metal-ethylenediamine-intercalated superconductors $\text{A}_x(\text{C}_2\text{H}_8\text{N}_2)_y\text{Fe}_2\text{-zSe}_2$ ($\text{A} = \text{Li}, \text{Na}$) with $T_c=45$ K," *Physica C-Superconductivity and Its Applications* **504**, 8 (2014).
- 49 Qing-Yan Wang, Zhi Li, Wen-Hao Zhang, Zuo-Cheng Zhang, Jin-Song Zhang, Wei Li, Hao Ding, Yun-Bo Ou, Peng Deng, Kai Chang, Jing Wen, Can-Li Song, Ke He, Jin-Feng Jia, Shuai-Hua Ji, Ya-Yu Wang, Li-Li Wang, Xi Chen, Xu-Cun Ma, and Qi-Kun Xue, "Interface-Induced High-Temperature Superconductivity in Single Unit-Cell FeSe Films on SrTiO_3 ," *Chin. Phys. Lett.* **29**, 037402 (2012).
- 50 Shaolong He, Junfeng He, Wenhao Zhang, Lin Zhao, Defa Liu, Xu Liu, Daixiang Mou, Yun-Bo Ou, Qing-Yan Wang, Zhi Li, Lili Wang, Yingying Peng, Yan Liu, Chaoyu Chen, Li Yu, Guodong Liu, Xiaoli Dong, Jun Zhang, Chuangtian Chen, Zuyan Xu, Xi Chen, Xucun Ma, Qikun Xue, and X.J. Zhou, "Phase diagram and electronic indication of high-temperature superconductivity at 65K insingle-layer FeSe film," *Nat. Mater.* **12**, 605 (2013).
- 51 S. Margadonna, Y. Takabayashi, M. T. McDonald, K. Kasperkiewicz, Y. Mizuguchi, Y. Takano, A. N. Fitch, E. Suard, and K. Prassides, "Crystal structure of the new FeSe_{1-x} superconductor," *Chem Commun (Camb)*, 5607 (2008).
- 52 T. M. McQueen, A. J. Williams, P. W. Stephens, J. Tao, Y. Zhu, V. Ksenofontov, F. Casper, C. Felser, and R. J. Cava, "Tetragonal-to-orthorhombic structural phase transition at 90 K in the superconductor $\text{Fe}_{1.01}\text{Se}$," *Phys. Rev. Lett.* **103**, 057002 (2009).
- 53 K. Nakayama, Y. Miyata, G. N. Phan, T. Sato, Y. Tanabe, T. Urata, K. Tanigaki, and T. Takahashi, "Reconstruction of band structure induced by electronic nematicity in an FeSe superconductor," *Phys. Rev. Lett.* **113**, 237001 (2014).
- 54 T. Shimojima, Y. Suzuki, T. Sonobe, A. Nakamura, M. Sakano, J. Omachi, K. Yoshioka, M. Kuwata-Gonokami, K. Ono, H. Kumigashira, A. E. Böhmer, F. Hardy, T. Wolf, C. Meingast, H. v Löhneysen, H. Ikeda, and K. Ishizaka, "Lifting of xz/yz orbital degeneracy at the structural transition in detwinned FeSe," *Phys. Rev. B* **90**, 121111R (2014).
- 55 S. H. Baek, D. V. Efremov, J. M. Ok, J. S. Kim, Jeroen van den Brink, and B. Buchner, "Orbital-driven nematicity in FeSe," *Nat. Mater.* **14**, 210 (2015).
- 56 X. H. Niu, R. Peng, H. C. Xu, Y. J. Yan, J. Jiang, D. F. Xu, T. L. Yu, Q. Song, Z. C. Huang, Y. X. Wang, B. P. Xie, X. F. Lu, N. Z. Wang, X. H. Chen, Z. Sun, and D. L. Feng, "Surface electronic structure and isotropic superconducting gap in $(\text{Li}_{0.8}\text{Fe}_{0.2})\text{OHFeSe}$," *Phys. Rev. B* **92**, 060504R (2015).
- 57 Lin Zhao, Aiji Liang, Dongna Yuan, Yong Hu, Defa Liu, Jianwei Huang, Shaolong He, Bing Shen, Yu Xu, Xu Liu, Li Yu, Guodong Liu, Huaxue Zhou, Yulong Huang, Xiaoli Dong, Fang Zhou, Kai Liu, Zhongyi Lu, Zhongxian Zhao, Chuangtian Chen, Zuyan Xu, and X. J. Zhou, "Common electronic origin of superconductivity in $(\text{Li},\text{Fe})\text{OHFeSe}$ bulk superconductor and single-layer FeSe/ SrTiO_3 films," *Nat. Commun.* **7**, 10608 (2016).
- 58 Xiaoli Dong, Kui Jin, Dongna Yuan, Huaxue Zhou, Jie Yuan, Yulong Huang, Wei Hua, Junliang Sun, Ping Zheng, Wei Hu, Yiyuan Mao, Mingwei Ma, Guangming Zhang, Fang Zhou, and Zhongxian Zhao, " $(\text{Li}_{0.84}\text{Fe}_{0.16})\text{OHFe}_{0.98}\text{Se}$ superconductor: Ion-exchange

synthesis of large single-crystal and highly two-dimensional electron properties," *Phys. Rev. B* **92**, 064515 (2015).

- 59 Huaxue Zhou, Shunli Ni, Jie Yuan, Jun Li, Zhongpei Feng, Xingyu Jiang, Yulong Huang, Shaobo Liu, Yiyuan Mao, Fang Zhou, Kui Jin, Xiaoli Dong, and Zhongxian Zhao, "Doping Mn into $(\text{Li}_{1-x}\text{Fe}_x)\text{OHFe}_{1-y}\text{Se}$ superconducting crystals via ion-exchange and ion-release/introduction syntheses," *Chin. Phys. B* **26**, 057402 (2017).
- 60 Y. Y. Mao, J. Li, Y. L. Huan, J. Yuan, Z. A. Li, K. Chai, M. W. Ma, S. L. Ni, J. P. Tian, S. B. Liu, H. X. Zhou, F. Zhou, J. Q. Li, G. M. Zhang, K. Jin, X. L. Dong, and Z. X. Zhao, "Electronic Phase Separation in Iron Selenide $(\text{Li,Fe})\text{OHFeSe}$ Superconductor System," *Chin. Phys. Lett.* **35**, 057402 (2018).
- 61 Dongna Yuan, Yulong Huang, Shunli Ni, Huaxue Zhou, Yiyuan Mao, Wei Hu, Jie Yuan, Kui Jin, Guangming Zhang, Xiaoli Dong, and Fang Zhou, "Synthesis of large FeSe superconductor crystals via ion release/introduction and property characterization," *Chin. Phys. B* **25**, 077404 (2016).
- 62 Shunli Ni, Wei Hu, Peipei Shen, Zhongxu Wei, Shaobo Liu, Dong Li, Jie Yuan, Li Yu, Kui Jin, Fang Zhou, Xiaoli Dong, and Zhongxian Zhao, "Different behavior of upper critical field in Fe_{1-x}Se single crystals," *Chinese Physics B* **28**, 127401 (2019).
- 63 Xiaoli Dong, Huaxue Zhou, Huaixin Yang, Jie Yuan, Kui Jin, Fang Zhou, Dongna Yuan, Linlin Wei, Jianqi Li, Xinqiang Wang, Guangming Zhang, and Zhongxian Zhao, "Phase Diagram of $(\text{Li}_{1-x}\text{Fe}_x)\text{OHFeSe}$: A Bridge between Iron Selenide and Arsenide Superconductors," *J. Am. Chem. Soc.* **137**, 66 (2015).
- 64 Dongna Yuan, Jie Yuan, Yulong Huang, Shunli Ni, Zhongpei Feng, Huaxue Zhou, Yiyuan Mao, Kui Jin, Guangming Zhang, Xiaoli Dong, Fang Zhou, and Zhongxian Zhao, "Observation of Ising spin-nematic order and its close relationship to the superconductivity in FeSe single crystals," *Phys. Rev. B* **94**, 060506R (2016).
- 65 Hualei Sun, Daniel N. Woodruff, Simon J. Cassidy, Genevieve M. Allcroft, Stefan J. Sedlmaier, Amber L. Thompson, Paul A. Bingham, Susan D. Forder, Simon Cartenet, Nicolas Mary, Silvia Ramos, Francesca R. Foronda, Benjamin H. Williams, Xiaodong Li, Stephen J. Blundell, and Simon J. Clarke, "Soft chemical control of superconductivity in lithium iron selenide hydroxides $\text{Li}_{1-x}\text{Fe}_x(\text{OH})\text{Fe}_{1-y}\text{Se}$," *Inorg. Chem.* **54**, 1958 (2015).
- 66 Y. L. Huang, Z. P. Feng, J. Yuan, W. Hu, J. Li, S. L. Ni, S. B. Liu, Y. Y. Mao, H. X. Zhou, H. B. Wang, F. Zhou, G.M. Zhang, K. Jin, X. L. Dong, and Z. X. Zhao, "Matrix-assisted fabrication and exotic charge mobility of $(\text{Li,Fe})\text{OHFeSe}$ superconductor films," *arXiv1711.02920* (2017).
- 67 Rustem Khasanov, Huaxue Zhou, Alex Amato, Zurab Guguchia, Elvezio Morenzoni, Xiaoli Dong, Guangming Zhang, and Zhongxian Zhao, "Proximity-induced superconductivity within the insulating $(\text{Li}_{0.84}\text{Fe}_{0.16})\text{OH}$ layers in $(\text{Li}_{0.84}\text{Fe}_{0.16})\text{OHFe}_{0.98}\text{Se}$," *Phys. Rev. B* **93**, 224512 (2016).
- 68 M. Smidman, G. M. Pang, H. X. Zhou, N. Z. Wang, W. Xie, Z. F. Weng, Y. Chen, X. L. Dong, X. H. Chen, Z. X. Zhao, and H. Q. Yuan, "Probing the superconducting gap structure of $(\text{Li}_{1-x}\text{Fe}_x)\text{OHFeSe}$," *Phys. Rev. B* **96**, 014504 (2017).
- 69 Zhaosheng Wang, Jie Yuan, J. Wosnitzer, Huaxue Zhou, Yulong Huang, Kui Jin, Fang Zhou, Xiaoli Dong, and Zhongxian Zhao, "The upper critical field and its anisotropy in $(\text{Li}_{1-x}\text{Fe}_x)\text{OHFe}_{1-y}\text{Se}$," *J. Phys-condens. Mat.* **29**, 025701 (2017).

- 70 J. P. Sun, P. Shahi, H. X. Zhou, Y. L. Huang, K. Y. Chen, B. S. Wang, S. L. Ni, N. N. Li, K. Zhang, W. G. Yang, Y. Uwatoko, G. Xing, J. Sun, D. J. Singh, K. Jin, F. Zhou, G. M. Zhang, X. L. Dong, Z. X. Zhao, and J. G. Cheng, "Reemergence of high-T-c superconductivity in the $(\text{Li}_{1-x}\text{Fe}_x)\text{OHFe}_{1-y}\text{Se}$ under high pressure," *Nat. Commun.* **9**, 380 (2018).
- 71 H. Xiao, T. Hu, H. X. Zhou, X. J. Li, S. L. Ni, F. Zhou, and X. L. Dong, "Probing the anisotropy of $(\text{Li}_{0.84}\text{Fe}_{0.16})\text{OHFe}_{0.98}\text{Se}$ by angular-dependent torque measurements," *Phys. Rev. B* **101**, 184520 (2020).
- 72 Zengyi Du, Xiong Yang, Hai Lin, Delong Fang, Guan Du, Jie Xing, Huan Yang, Xiyu Zhu, and Hai-Hu Wen, "Scrutinizing the double superconducting gaps and strong coupling pairing in $(\text{Li}_{1-x}\text{Fe}_x)\text{OHFeSe}$," *Nat. Commun.* **7**, 10565 (2016).
- 73 Xiuquan Zhou, Christopher K. H. Borg, Jeffrey W. Lynn, Shanta R. Saha, Johnpierre Paglione, and Efrain E. Rodriguez, "The preparation and phase diagrams of $(^7\text{Li}_{1-x}\text{Fe}_x\text{OD})\text{FeSe}$ and $(\text{Li}_{1-x}\text{Fe}_x\text{OH})\text{FeSe}$ superconductors," *Journal of Materials Chemistry C* **4**, 3934 (2016).
- 74 Bingying Pan, Yao Shen, Die Hu, Yu Feng, J. T. Park, A. D. Christianson, Qisi Wang, Yiqing Hao, Hongliang Wo, Zhiping Yin, T. A. Maier, and Jun Zhao, "Structure of spin excitations in heavily electron-doped $\text{Li}_{0.8}\text{Fe}_{0.2}\text{ODFeSe}$ superconductors," *Nat. Commun.* **8**, 123 (2017).
- 75 Mingwei Ma, Lichen Wang, Philippe Bourges, Yvan Sidis, Sergey Danilkin, and Yuan Li, "Low-energy spin excitations in $(\text{Li}_{0.8}\text{Fe}_{0.2})\text{ODFeSe}$ superconductor studied with inelastic neutron scattering," *Phys. Rev. B* **95**, 100504R (2017).
- 76 Mingqiang Ren, Yajun Yan, Xiaohai Niu, Ran Tao, Die Hu, Rui Peng, Binping Xie, Jun Zhao, Tong Zhang, and Dong-Lai Feng, "Superconductivity across Lifshitz transition and anomalous insulating state in surface K-dosed $(\text{Li}_{0.8}\text{Fe}_{0.2}\text{OH})\text{FeSe}$," *Science Advances* **3**, e1603238 (2017).
- 77 Yue Sun, Sunseng Pyon, Run Yang, Xianggang Qiu, Jiajia Feng, Zhixiang Shi, and Tsuyoshi Tamegai, "Deviation from Canonical Collective Creep Behavior in $\text{Li}_{0.8}\text{Fe}_{0.2}\text{OHFeSe}$," *J. Phys. Soc. Jpn.* **88**, 034703 (2019).
- 78 Xiaolei Yi, Lingyao Qin, Xiangzhuo Xing, Bencheng Lin, Meng Li, Yan Meng, Mingxiang Xu, and Zhixiang Shi, "Synthesis of $(\text{Li}_{1-x}\text{Fe}_x)\text{OHFeSe}$ and FeSe single crystals without using selenourea via a hydrothermal method," *J. Phys. Chem. Solids* **137**, 109207 (2020).
- 79 Christopher K. H. Borg, Xiuquan Zhou, Christopher Eckberg, Daniel J. Campbell, Shanta R. Saha, Johnpierre Paglione, and Efrain E. Rodriguez, "Strong anisotropy in nearly ideal tetrahedral superconducting FeS single crystals," *Phys. Rev. B* **93**, 094522 (2016).
- 80 G. Yu, G. Y. Zhang, G. H. Ryu, and C. T. Lin, "Structure and superconductivity of $(\text{Li}_{1-x}\text{Fe}_x)\text{OHFeSe}$ single crystals grown using $\text{A}_x\text{Fe}_{2-y}\text{Se}_2$ ($\text{A} = \text{K}, \text{Rb}, \text{and Cs}$) as precursors," *J Phys Condens Matter* **28**, 015701 (2016).
- 81 Hai Lin, Yufeng Li, Qiang Deng, Jie Xing, Jianzhong Liu, Xiyu Zhu, Huan Yang, and Hai-Hu Wen, "Multiband superconductivity and large anisotropy in FeS crystals," *Phys. Rev. B* **93**, 144505 (2016).
- 82 Xiaolei Yi, Chunlei Wang, Qingbin Tang, Tao Peng, Yang Qiu, Junqi Xu, Haibin Sun, Yongsong Luo, and Benhai Yu, "Vortex phase transition and anisotropy behavior of optimized $(\text{Li}_{1-x}\text{Fe}_x\text{OH})\text{FeSe}$ single crystals," *Supercond. Sci. Tech.* **29**, 105015 (2016).

- 83 Brandon Wilfong, Xiuquan Zhou, Huafei Zheng, Navneeth Babra, Craig M. Brown, Jeffrey W. Lynn, Keith M. Taddei, Johnpierre Paglione, and Efrain E. Rodriguez, "Long-range magnetic order in hydroxide-layer-doped $(\text{Li}_{1-x-y}\text{Fe}_x\text{Mn}_y\text{OD})\text{FeSe}$," *Physical Review Materials* **4**, 034803 (2020).
- 84 Jeffrey W. Lynn, Xiuquan Zhou, Christopher K. H. Borg, Shanta R. Saha, Johnpierre Paglione, and Efrain E. Rodriguez, "Neutron investigation of the magnetic scattering in an iron-based ferromagnetic superconductor," *Phys. Rev. B* **92**, 060510R (2015).
- 85 Ursula Pachmayr, Fabian Nitsche, Hubertus Luetkens, Sirko Kamusella, Felix Brueckner, Rajib Sarkar, Hans-Henning Klauss, and Dirk Johrendt, "Coexistence of 3d-ferromagnetism and superconductivity in $[(\text{Li}_{1-x}\text{Fe}_x)\text{OH}](\text{Fe}_{1-y}\text{Li}_y)\text{Se}$," *Angew. Chem. Int. Edit.* **54**, 293 (2015).
- 86 A. E. Böhmer, F. Hardy, F. Eilers, D. Ernst, P. Adelman, P. Schweiss, T. Wolf, and C. Meingast, "Lack of coupling between superconductivity and orthorhombic distortion in stoichiometric single-crystalline FeSe," *Phys. Rev. B* **87**, 180505R (2013).
- 87 Dmitriy Chareev, Evgeniy Osadchii, Tatiana Kuzmicheva, Jiunn-Yuan Lin, Svetoslav Kuzmichev, Olga Volkova, and Alexander Vasiliev, "Single crystal growth and characterization of tetragonal FeSe_{1-x} superconductors," *Cryst. Eng. Comm* **15**, 1989 (2013).
- 88 Mingwei Ma, Dongna Yuan, Yue Wu, Huaxue Zhou, Xiaoli Dong, and Fang Zhou, "Flux-free growth of large superconducting crystal of FeSe by traveling-solvent floating-zone technique," *Supercond. Sci. Tech.* **27**, 122001 (2014).
- 89 Sahana Röfler, Cevriye Koz, Lin Jiao, Ulrich K. Röfler, Frank Steglich, Ulrich Schwarz, and Steffen Wirth, "Emergence of an incipient ordering mode in FeSe," *Phys. Rev. B* **92**, 060505R (2015).
- 90 Yue Sun, Sunseng Pyon, and Tsuyoshi Tamegai, "Electron carriers with possible Dirac-cone-like dispersion in $\text{FeSe}_{1-x}\text{S}_x$ ($x=0$ and 0.14) single crystals triggered by structural transition," *Phys. Rev. B* **93**, 104502 (2016).
- 91 T. Urata, Y. Tanabe, K. K. Huynh, Y. Yamakawa, H. Kontani, and K. Tanigaki, "Superconductivity pairing mechanism from cobalt impurity doping in FeSe: Spin ($s\pm$) or orbital ($s++$) fluctuation," *Phys. Rev. B* **93**, 014507 (2016).
- 92 M. C. Rahn, R. A. Ewings, S. J. Sedlmaier, S. J. Clarke, and A. T. Boothroyd, "Strong $(\pi,0)$ spin fluctuations in $\beta\text{-FeSe}$ observed by neutron spectroscopy," *Phys. Rev. B* **91**, 180501R (2015).
- 93 U. Pachmayr, N. Fehn, and D. Johrendt, "Structural transition and superconductivity in hydrothermally synthesized FeX ($X = \text{S}, \text{Se}$)," *Chem. Commun.* **52**, 194 (2016).
- 94 Qisi Wang, Yao Shen, Bingying Pan, Yiqing Hao, Mingwei Ma, Fang Zhou, P. Steffens, K. Schmalzl, T. R. Forrest, M. Abdel-Hafiez, Xiaojia Chen, D. A. Chareev, A. N. Vasiliev, P. Bourges, Y. Sidis, Huibo Cao, and Jun Zhao, "Strong interplay between stripe spin fluctuations, nematicity and superconductivity in FeSe," *Nat. Mater.* **15**, 159 (2016).
- 95 Kazumasa Iida, Jens Haenisch, Chiara Tarantini, Fritz Kurth, Jan Jaroszynski, Shinya Ueda, Michio Naito, Ataru Ichinose, Ichiro Tsukada, Elke Reich, Vadim Grinenko, Ludwig Schultz, and Bernhard Holzapfel, "Oxypnictide $\text{SmFeAs}(\text{O},\text{F})$ superconductor: a candidate for high-field magnet applications," *Scientific Reports* **3**, 2139 (2013).

- 96 Weidong Si, Su Jung Han, Xiaoya Shi, Steven N. Ehrlich, J. Jaroszynski, Amit Goyal, and Qiang Li, "High current superconductivity in FeSe_{0.5}Te_{0.5}-coated conductors at 30 tesla," Nat. Commun. **4**, 1347 (2013).
- 97 F. Kurth, C. Tarantini, V. Grinenko, J. Hänisch, J. Jaroszynski, E. Reich, Y. Mori, A. Sakagami, T. Kawaguchi, J. Engelmann, L. Schultz, B. Holzapfel, H. Ikuta, R. Hühne, and K. Iida, "Unusually high critical current of clean P-doped BaFe₂As₂ single crystalline thin film," Appl. Phys. Lett. **106**, 072602 (2015).
- 98 A. Xu, J. J. Jaroszynski, F. Kametani, Z. Chen, D. C. Larbalestier, Y. L. Viouchkov, Y. Chen, Y. Xie, and V. Selvamanickam, "Angular dependence of J_c for YBCO coated conductors at low temperature and very high magnetic fields," Supercond. Sci. Tech. **23**, 014003 (2010).

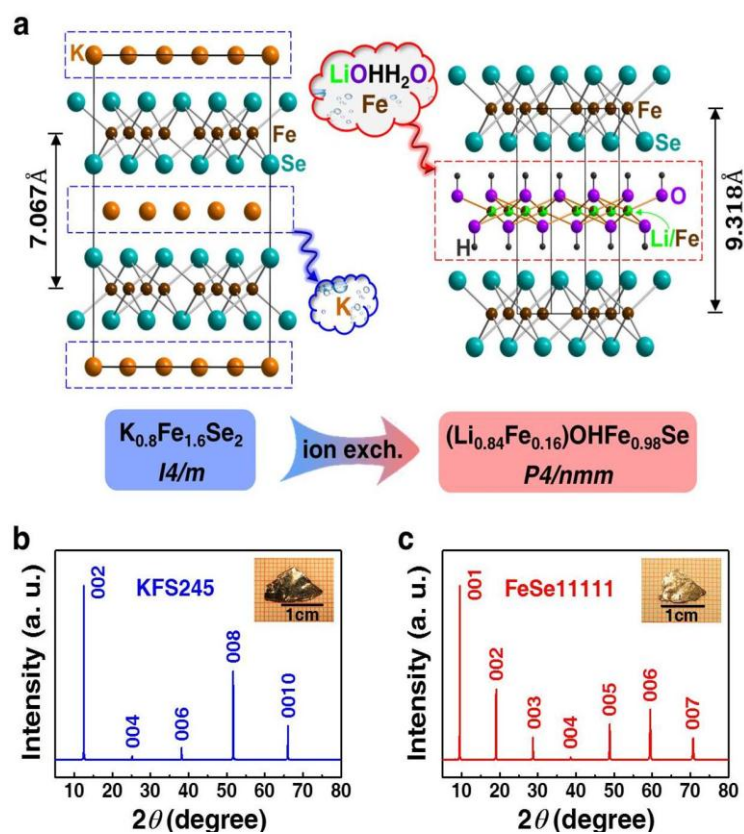


Figure 1 Illustration of hydrothermal ion-exchange growth of (Li,Fe)OHFeSe crystals [58].

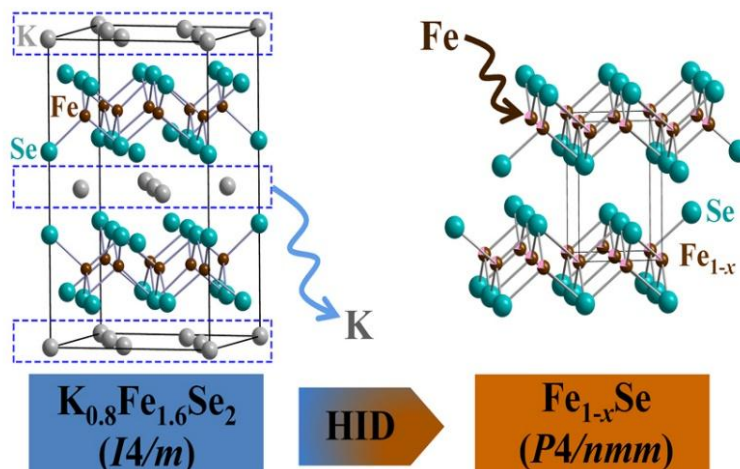


Figure 2 Schematic illustration of the hydrothermal ion-deintercalation method. During the HID process, Fe_{1-x}Se single crystals are derived from the readily obtainable phase-pure matrix single crystals of $\text{K}_{0.8}\text{Fe}_{1.6}\text{Se}_2$. The original interlayer K ions and Fe vacancies (20 % in amount) in $\text{K}_{0.8}\text{Fe}_{1.6}\text{Se}_2$ were completely de-intercalated and substantially reduced, respectively, yielding the target single crystals of phase-pure Fe_{1-x}Se [9,61,62].

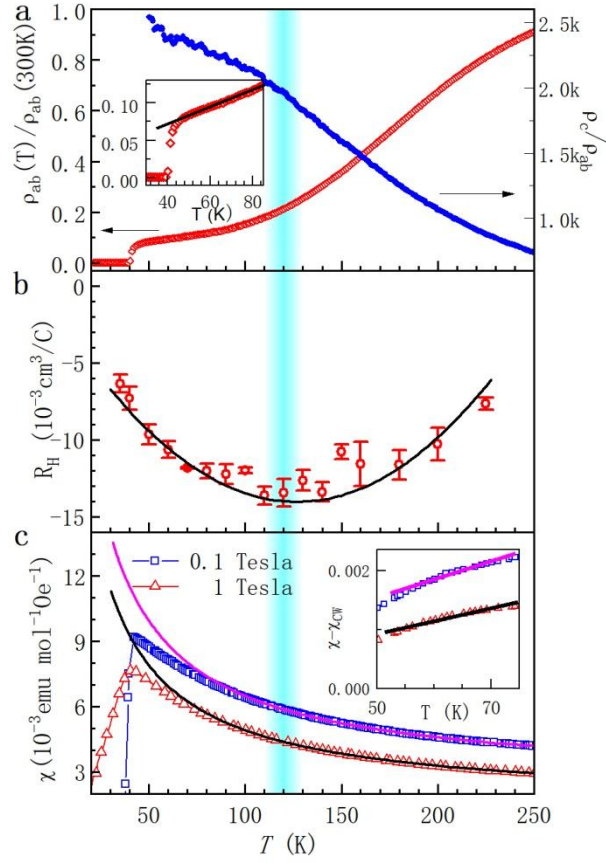


Figure 3 The electrical transport and magnetic properties of $(\text{Li}_{0.84}\text{Fe}_{0.16})\text{OHFe}_{0.98}\text{Se}$ single crystal [58]. (a) The in-plane electrical resistivity and the ratio of out-of-plane to in-plane resistivity as functions of temperature. The inset shows the linear resistivity below the Hall-dip T^* down to T_c . (b) The temperature dependence of in-plane Hall coefficient shows a dip feature around $T^* \sim 120$ K. (c) The temperature dependencies of static magnetic susceptibility under magnetic fields along c -axis. A deviation from the Curie-Weiss law is clearly visible below the Hall-dip T^* . After subtracting the Curie-Weiss term (the solid fitted curves) from the $(\text{Li}_{0.84}\text{Fe}_{0.16})\text{OH}$ -blocks, a nearly linear magnetic susceptibility from the FeSe-blocks is obvious (the inset).

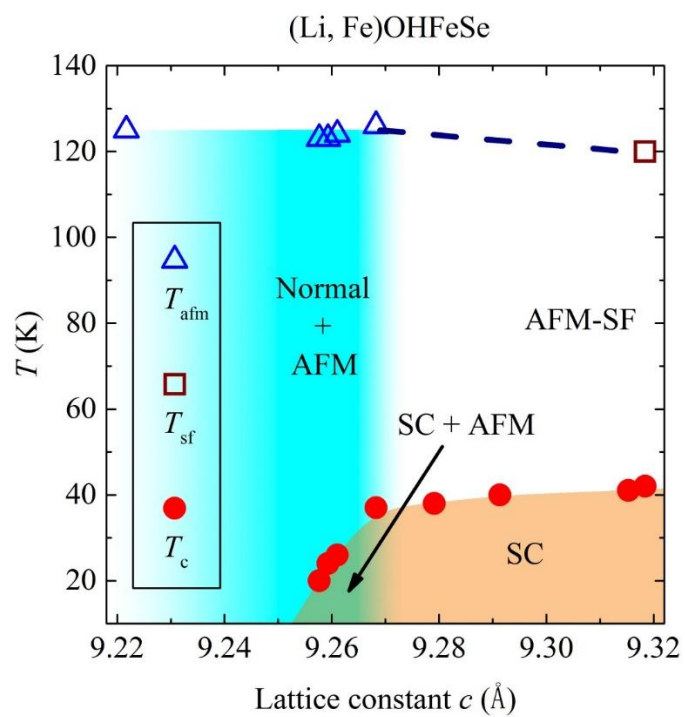


Figure 4 Electronic phase diagram of (Li,Fe)OHFeSe system [60,63].

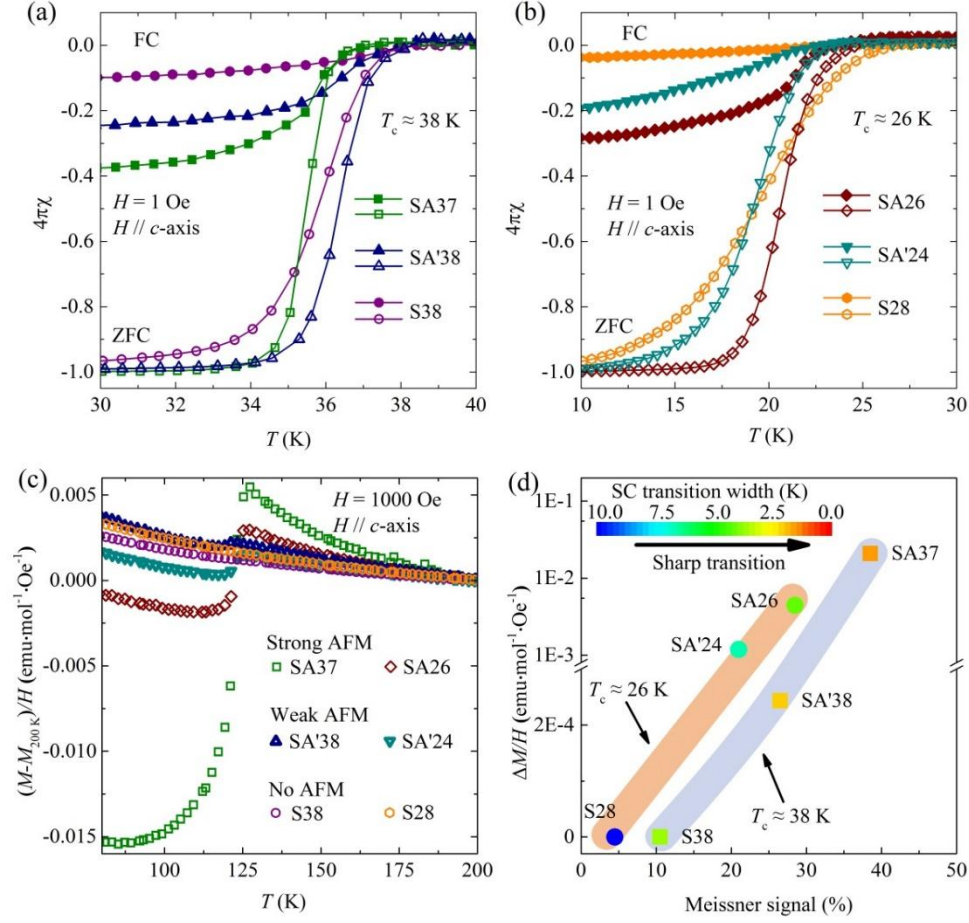


Figure 5 (a) and (b) Temperature dependence of static magnetic susceptibility near the superconducting transitions, for the two sets of superconducting (Li,Fe)OHFeSe single crystals. (c) Antiferromagnetic (AFM) transition at ~ 125 K is detectable for the superconducting ($T_c < \sim 38$ K) samples and non-superconducting samples. (d) The corresponding AFM signal size and the SC Meissner signal size are positively correlated [60].

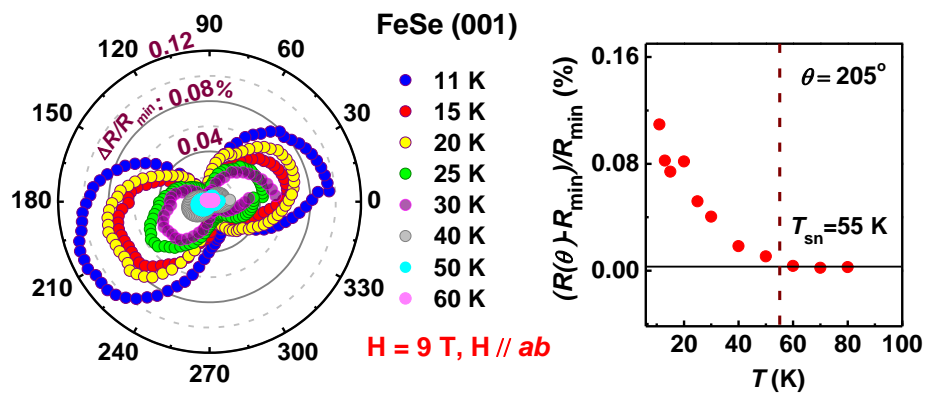


Figure 6 Temperature dependences of the angular-dependent magnetoresistance of FeSe crystal ($T_c = 7.6$ K), showing the twofold rotational symmetry below $T_{\text{sn}} \sim 55$ K [64].

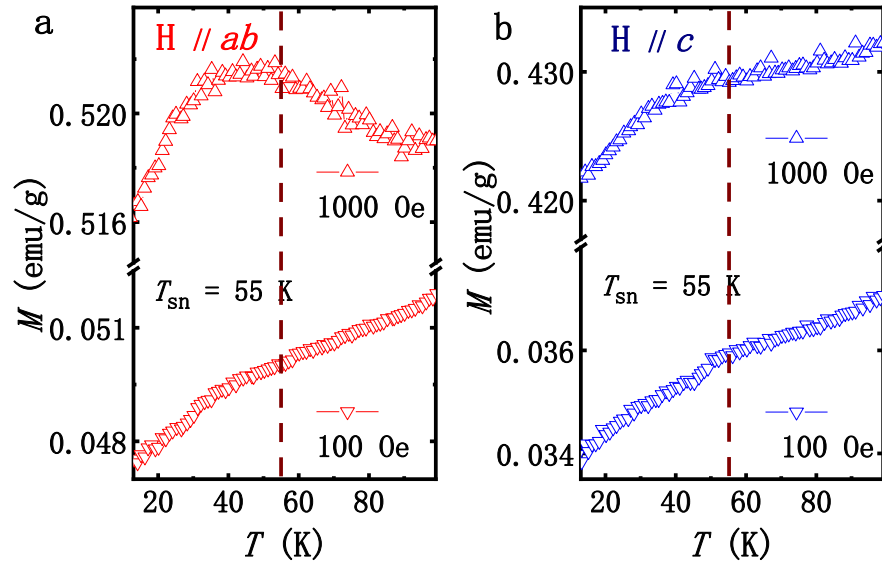


Figure 7 Temperature dependence of the static magnetization around 55 K under the in-plane and out-of-plane fields for the FeSe crystal shown in Fig. 6. [61]

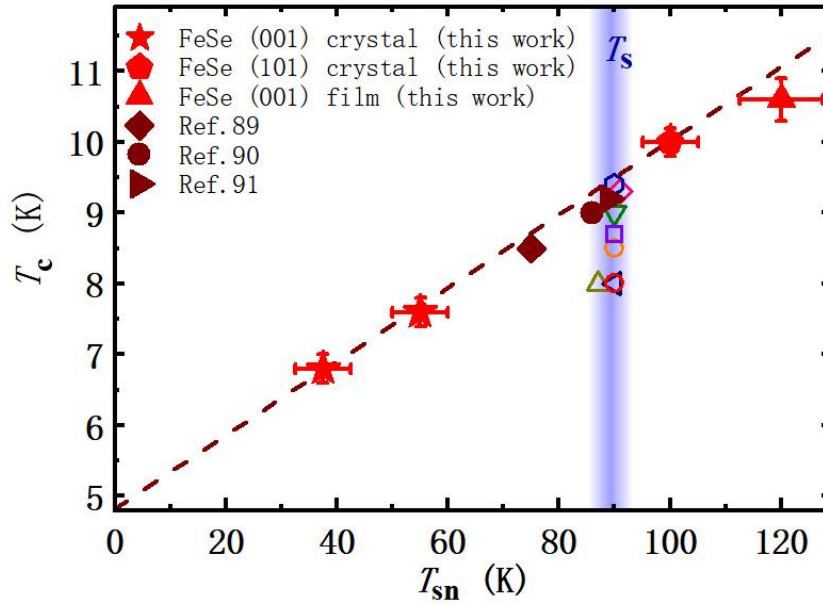


Figure 8 The universal linear relationship between the superconducting transition temperature (T_c) and the field-induced spin-nematic ordering temperature (T_{sn}) among various FeSe samples (the solid symbols) [64]. The hollow symbols in the vertical blue-shaded area represent the structure phase transition temperatures by the x-ray or neutron diffractions on various FeSe samples of different T_c 's [30,52,55,86,92-94].

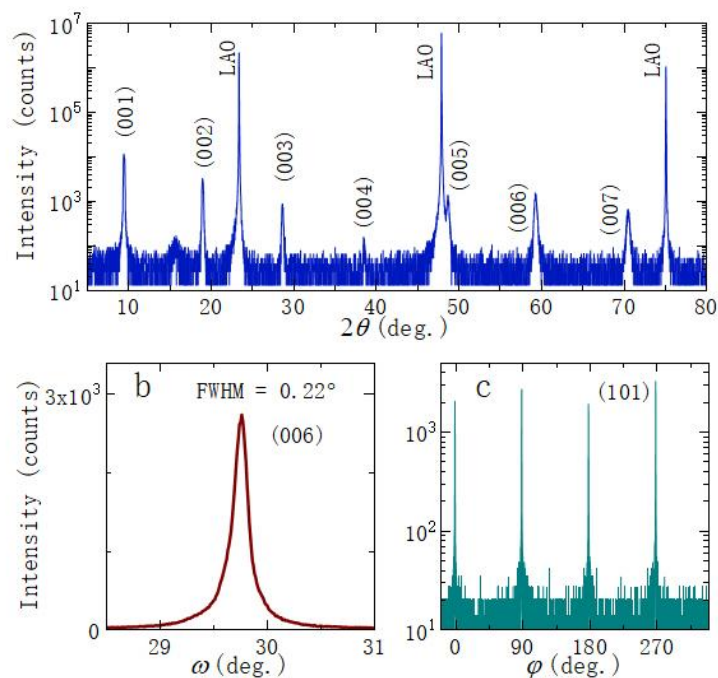


Figure 9 XRD characterizations of the (Li,Fe)OHFeSe film on the LaAlO₃ (LAO) substrate. (a) The θ - 2θ scan shows only (00 l) peaks. (b) The rocking curve of (006) reflection with an FWHM of 0.22° . (c) The ϕ -scan of the (101) plane. The uniform 4-fold symmetry reveals an excellent epitaxial growth [16].

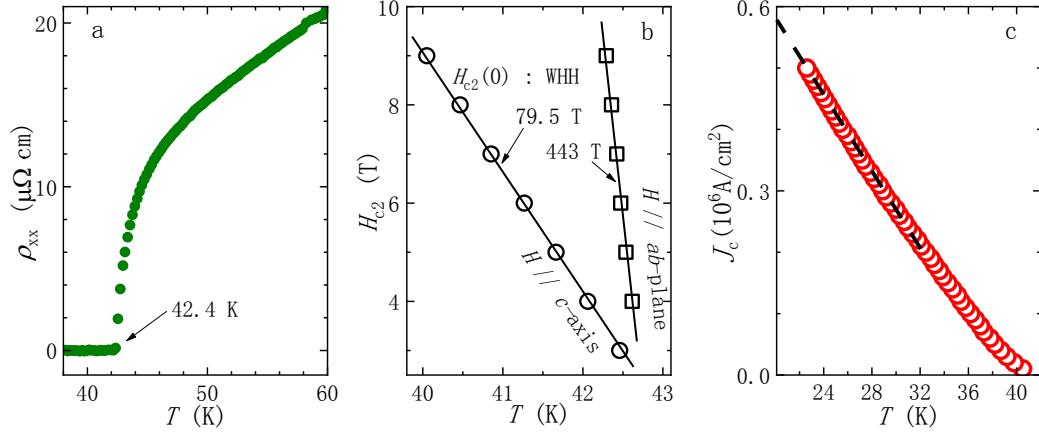


Figure 10 High superconducting critical parameters for (Li,Fe)OHFeSe film. (a) Temperature dependence of in-plane resistivity, with the onset of zero resistivity at 42.4 K. (b) Temperature dependence of $H_{c2}(T)$ along the c -axis (circle) and within the ab plane (square). (c) The temperature dependence of J_c , exceeding 0.5 MA/cm^2 at 20K [16].

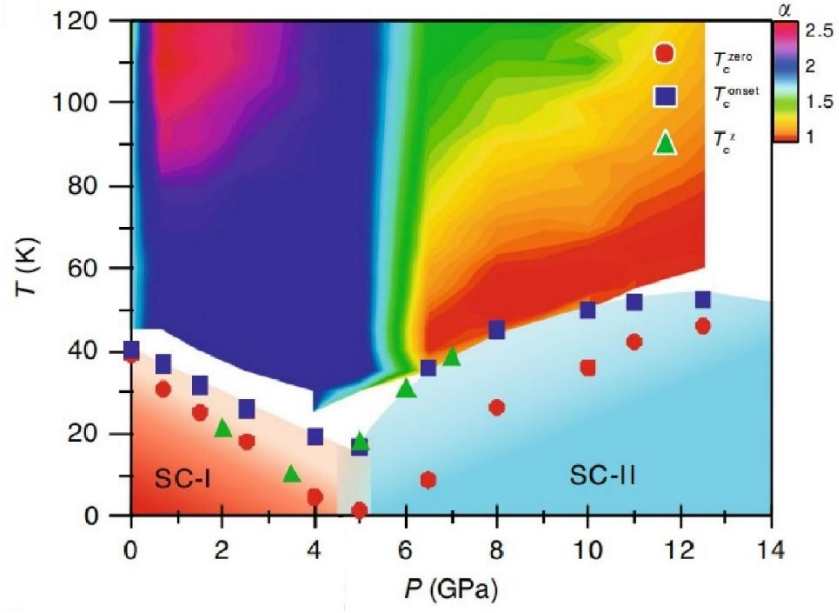


Figure 11 Temperature-pressure phase diagram of $(\text{Li}_{0.84}\text{Fe}_{0.16})\text{OHFe}_{0.98}\text{Se}$ single crystal [70]. Pressure-dependence of T_c and a contour color plot of the normal-state resistivity exponent α up to 12.5 GPa are shown.

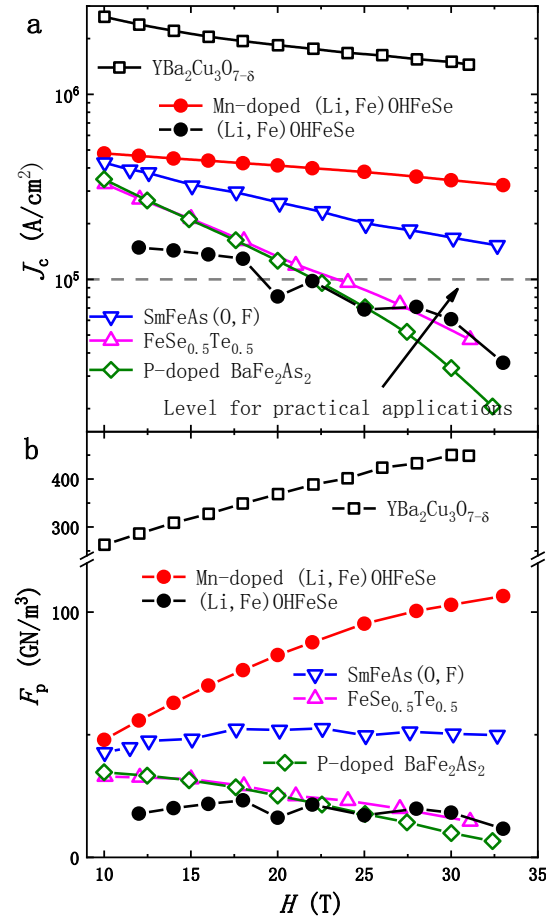


Figure 12 Magnetic field dependence of J_c (a) and F_p (b) of several superconductors [17], including Mn-doped and pure (Li,Fe)OHFeSe films at 5 K, SmFeAs(O,F) films [95], $\text{FeSe}_{0.5}\text{Te}_{0.5}$ films [96], P-doped BaFe_2As_2 films [97], and $\text{YBa}_2\text{Cu}_3\text{O}_{7-\delta}$ wires [98] at 4.2 K under c-axis fields.